Polymerization of Olefins Through Heterogeneous Catalysis— V. Gas-Liquid Mass Transfer Limitations in Liquid Slurry Reactors

S. FLOYD,* R.A. HUTCHINSON, and W. H. RAY, *Department of Chemical Engineering, University of Wisconsin, Madison, Wisconsin 53706*

Synopsis

Many processes for polymerization of olefins employ laboratory, pilot plant, or full-scale liquid-phase polymerization reactors with monomer introduced as a gas. Criteria for the presence of gas-liquid mass transfer resistance in these systems are determined in terms of observed reaction rate or loading of a heterogeneous catalyst of given intrinsic activity. The effects of variables such as reactor size and configuration, temperature, and soluble polymer are also examined. The equilibrium monomer concentrations of ethylene in hexane and propylene in heptane are calculated through a modified Benedict-Webb-Rubin equation, and some calculations for ethylene-propylene mixtures are tabulated. The general methodology for predicting gas-liquid mass transfer resistance is readily extendible to copolymerization systems.

INTRODUCTION

In many polymerization reactors, the monomer is introduced as a gas which must dissolve in the continuous liquid phase before participating in the polymerization. Some advantages of this mode of operation are high space–time yield and good temperature control.[1] However, if the rate of polymerization is sufficiently fast, gas-liquid mass transfer can become the rate-limiting step. In this case, catalyst-intrinsic activities will be disguised by this mass transfer limitation. Thus, to insure consistency of laboratory, pilot plant, and industrial scale kinetic data, it is essential to estimate the effect of gas-liquid mass transfer on the observed polymerization behavior.

Some recent reviews[2,3] contain much useful information for the design of three-phase slurry reactors. In particular, if the energy required for solids suspension is small, many of the principles for the design of gas-liquid reactors will be directly applicable. In the present paper, we shall specifically deal with ethylene and propylene polymerization in liquid slurry. However, the correlations and methodology readily apply to other suspension polymerization systems as well as more general polymerization reactors, for example, emulsion polymerization reactors where the monomer is fed as a gas. Experimentally, it is possible to establish the presence of a gas-liquid mass transfer resistance for a given catalyst loading simply by changing the agitation rate.

*Present address: Exxon Chemical Co., Linden, New Jersey 07036.

Journal of Applied Polymer Science, Vol. 32, 5451–5479 (1986)
© 1986 John Wiley & Sons, Inc. CCC 0021-8995/86/065451-29$04.00

By means of a reciprocal plot of polymerization rate versus loading, the mass transfer resistance can be determined, and through appropriate corrections, the true kinetic parameters can be obtained.[5,6] However, the motivation for the present work is to provide the researcher with a means of estimating *a priori* the mass transfer resistance at a given loading or observed rate. This should be of use in choosing catalyst loadings at each stage of development and aid reactor design, eliminating the necessity for costly trial and error experiments. In addition, the results will be useful in interpreting existing kinetic data—in order to estimate the likely effect of mass transfer limitations on the reported results.

To illustrate the results, we shall choose as practical examples three common types of reactor: (i) a glass reactor of a type used for kinetic testing in the laboratory,[7,8] operating at or near atmospheric pressure and relying on a magnetic stir-bar for agitation, (ii) a half-gallon pilot plant reactor, operating at 7–15 atm, with or without sparged gas, and finally (iii) a full-scale industrial reactor of 20,000 gallons, operating at 15–35 atm. We will derive and present relations for gas-liquid mass transfer resistance which are independent of the catalyst system. However, some results will also be presented for catalyst systems of specific activity. The symbols which will be used throughout this paper are defined in the Appendix.

GAS-LIQUID MASS TRANSFER CORRELATIONS

In this section, we shall consider the prediction of mass transfer rates under specific operating conditions. Estimation of the mass transfer resistance requires knowledge of the equilibrium solubility of monomer in the bulk liquid, M_{eq}, as well as the volumetric mass transfer coefficient $k_\ell a$, which is the product of the liquid side mass transfer coefficient k_ℓ, and the interfacial area of gas per unit volume, a. For monomer gas present in high concentration, there is negligible gas side mass transfer resistance, and the degree of mixing of the gas phase is not a consideration. Complete mixing in the liquid phase will be assumed, although this is not always achieved for large reactors or liquids of high viscosity.[9,10] With $k_\ell a$ and M_{eq} known, the mass transfer resistance may be calculated for an observed volumetric polymerization rate R_{vob} [mol/L/h]. Thus, a quasi-steady-state material balance yields

$$k_l a(M_{eq} - M_b) = R_{vob} \tag{1}$$

or rearranging

$$\frac{M_b}{M_{eq}} = \frac{k_l a - R_{vob}/M_{eq}}{k_l a} \tag{2}$$

If we recall that for a given catalyst with specific observed activity, k_{cat} [L/g-cat/h] and loading W [g-cat/L] the observed reaction rate per unit volume of reactor R_{vob} [mol monomer converted/L.h] is

$$R_{vob} = k_{cat} W M_b = R_{ob} W/\mathrm{MW} \tag{3}$$

where $R_{ob} = k_{cat} M_b \mathrm{MW}$ is the observed production rate of the catalyst

(g-pol/g-cat.h), and k_{cat} is the catalyst activity which includes *particle* mass transfer limitations, i.e.; $k_{cat} = \frac{k_p C^*}{\rho_c}\eta$ overall. Similarly the "ideal" volumetric reaction rate (in the absence of any gas-liquid mass transfer resistance) is

$$R_{vid} = k_{cat} W M_{eq} = R_{id} \frac{W}{MW} \tag{4}$$

where $R_{id} = k_{cat} M_{eq} MW$ is the ideal production rate of the catalyst (g-pol/g-cat.h).

Hence,

$$\frac{M_b}{M_{eq}} = \frac{R_{vob}}{R_{vid}} = \frac{k_l a}{k_{cat} W + k_l a} \tag{5}$$

Note that Eq. (2) provides a prediction of the mass transfer resistance for a given observed polymerization rate, while Eq. (5) yields the relative rates of polymerization under actual vs. ideal conditions for a given catalyst and loading.

In the literature, a number of correlations are available for $k_\ell a$, and also for k_l and a individually. The interfacial area a is related to the gas holdup H_o and the mean bubble diameter d_b through the relationship[9]

$$a = \frac{6H_o}{d_b} \tag{6}$$

where one may use correlations for d_b. Actually, both the bubble diameter and the interfacial area are a function of the distance from the impeller. This is because the energy dissipation in the reactor is not uniform.[11] Thus, disintegration occurs at the impeller, while coalescence takes place far away.[11-13] For this reason, the average interfacial area decreases with tank height, when $H/D_T > 10$. However, for the reactors considered here, $H/D_T \sim 1$. Hence, the interfacial area will be considered as uniform throughout the reactor. It is important to note that most correlations have been derived for sparged, agitated tanks and aqueous media. Hence, the applicability of these correlations to olefin polymerization must be carefully examined. In two recent reviews, Gollakota[14] and Van't Riet[9] stated that the most important variables determining $k_\ell a$ in mixing vessels are the power per unit volume (P/V), the superficial gas velocity (v_s), the ionic strength, the solution viscosity, and the surface tension. However, the impact of these variables may be very different for different systems, geometries, and ranges of the variables.[9,12,15-17] For instance, P/V is an important parameter when $H/D_T < 2$, but for large H/D_T, it becomes relatively unimportant.[9] At the same P/V, the stirrer type and even the number of stirrers is frequently unimportant. The simplest correlations for $k_\ell a$ involve only power per unit volume and the superficial gas velocity, but these correlations will be rejected because they are applicable only for the specific systems for which they were derived (usually the air-water system). More general correlations for $k_\ell a$ in sparged,

agitated systems are those of Yagi and Yoshida[16]

$$k_\ell a = 0.06 \frac{D_\ell}{D_I^{1.68}} \left(\frac{\mu_\ell}{\sigma_\ell} \right)^{0.6} \mathrm{Sc}_\ell \mathrm{Re}_s^{1.5} \mathrm{Fr}^{0.19} \mathrm{N}^{0.32} v_s^{0.28} \tag{7}$$

and Judat:[18]

$$k_\ell a = 9.85 \times 10^{-4} D_I^{0.6} \mathrm{N}^{1.2} g^{-0.053} \nu_\ell^{-0.45} Q^{0.76} D_T^{-0.72} (F_1 F_2)^{-0.6} \tag{8}$$

$$F_1 = 1 + 4.55 \times 10^3 (g D_I^3 / \nu_\ell^2)^{-1/3} \tag{8a}$$

$$F_2 = \left[D_T/D_I + 0.0396 (D_T/D_I)^3 \right]^{5/3} \tag{8b}$$

In these correlations, P/V does not appear directly, but enters through N, the agitation rate. For k_ℓ, in sparged, agitated vessels, Calderbank[19] has given a correlation:

$$k_\ell = 0.42 \left[\frac{(\rho_\ell - \rho_g) \mu_\ell g}{\rho_\ell^2} \right]^{1/3} Sc_\ell^{-1/2} \tag{9}$$

which is applicable to bubbles of greater than 2mm diameter. Most workers appear to agree that such bubbles are formed in aeration of pure liquids,[15,19-21] while small bubbles occur in electrolyte solutions.[9,14,15,19]. However, traces of surface-active compounds can result in a reduction in bubble size,[20] and increase in surface area.[22] For the interfacial area, Calderbank[22] presents a correlation

$$a_o = 230 \frac{(P/V)^{0.4} \rho_\ell^{0.2}}{\sigma_\ell^{0.6}} v_s^{1/2} \tag{10}$$

which is applicable at relatively low agitation rates. For higher agitation rates, specifically, for

$$\xi = \mathrm{Re}_s^{0.7} \left(\frac{N D_I}{v_s} \right)^{0.3} > 10{,}000 \tag{11}$$

a correction for surface aeration is required. This correction was approximated[23] as

$$\frac{a}{a_o} = 1.16 - 2.53 \times 10^{-5} \xi + 1.00 \times 10^{-9} \xi^2 \tag{12}$$

At high agitation rates, (12) can lead to increases in the interfacial area by a factor of 2 or more, so surface aeration is not a small effect.[19]

While the above correlations are applicable to sparged reactors, here, we are also concerned with unsparged vessels. Unfortunately, no sufficiently general correlation for $k_\ell a$ appears to have been proposed for these. Hence, we must

resort to a correlation for k_ℓ for a free surface, in conjunction with an assumed liquid surface area. For a free surface, Kozinski and King[24] presented a semitheoretical correlation

$$k_\ell = 0.25\left(\frac{P}{V}\right)^{1/4}\left(\frac{\mu_\ell}{\rho_\ell^2}\right)^{1/4} Sc_\ell^{-3/4} \tag{13}$$

(c.g.s. units) which was found to agree to within an order of magnitude with the data of several early works. However, they suggest that a significant correction for bubble entrainment to the area of the main free surface is necessary in order to harmonize this correlation with the $k_\ell a$ values they obtained experimentally. Calderbank[20] has presented a very similar correlation, but it seems to have been verified only for solid-liquid and liquid-liquid systems.

$$k_\ell = 0.13\left(\frac{P}{V}\right)^{1/4}\left(\frac{\mu_\ell}{\rho_\ell^2}\right)^{1/4} \mathrm{Sc}_\ell^{-2/3} \tag{14}$$

This can also be expressed as[23]

$$k_\ell = 0.13 N_p^{1/4}\mathrm{Re}_s^{3/4}\mathrm{Sc}_\ell^{1/3}\left(\frac{D_I^3}{V}\right)^{1/4}\frac{D_\ell}{D_I} \tag{15}$$

Equation (15) was used by Brockmeier and Rogan,[8] fixing the value of N_P at 0.364, applicable to the turbulent region. However, it seems reasonable to assume that a correlation for k_ℓ for a solid-liquid system might be somewhat conservative for a gas-liquid system, in which surface oscillations could lead to increased mass transfer.[25] Hence, in place of (14), the theoretically derived correlation of Lamont and Scott[25]

$$k_\ell = 0.4\left(\frac{P}{V}\right)^{1/4}\left(\frac{\mu_\ell}{\rho_\ell^2}\right)^{1/4} \mathrm{Sc}^{-1/2} \tag{16}$$

would seem more appropriate. This correlation is very similar to (13) and (14), but has a leading coefficient of 0.4 and a Schmidt exponent of $-1/2$, and thus predicts higher k_ℓ values. All these correlations display a dependence on a $1/4$ power of the power input, suggesting that the turbulence of the liquid (surface renewal) is indeed important. Other workers found that k_ℓ in unsparged vessels depends on the agitation rate with an exponent of roughly 1[14,26]to as high as 2.5.[27] Russian investigators have found an exponent of 2.5 for the oxygen transfer rate in a surface aerator.[28] For the area of contact between gas and liquid in unsparged systems, the contribution due to formation of a vortex was considered. For this purpose, an approximate relation presented by Tsao[29]

$$\mathrm{H}_v/\mathrm{H} = 2.5 \times 10^{-3}\mathrm{N}^2 \tag{17}$$

was used to estimate the vortex depth, and a correction was made to the area

of the main free interface assuming a vortex of parabolic shape. This correction caused the surface area to approximately double between 300 and 1000 rpm. In summary, the equations chosen for the determination of the mass transfer resistance were Eqs. (7), (8) and a combination of (9) with (10)–(12) for sparged vessels, and Eqs. (16) and (17) for unsparged vessels.

Some additional assumptions peculiar to the present problem will now be discussed. All of the correlations selected above are for two-phase (gas-liquid) systems, not slurries. Hence, the question of the effect of solids on the individual fluid properties, as well as the mass transfer coefficients, obviously arises. Fortunately, for moderate solids concentrations (up to around 30 wt%), the effects on $k_\ell a$ do not appear to be pronounced.[14,30] Some workers[14,31] have shown that k_ℓ or $k_\ell a$ increases slightly (10–20%) with the presence of small amounts of solids. This might be due to breakup of bubbles by particles, resulting in higher surface area.[33] However, at solids concentrations above 30–40%,[14,30-34] the interfacial area in sparged vessels decreases considerably. It has also been observed that for non-Newtonian fluids, gas dispersion near the impeller is reduced considerably compared to Newtonian fluids.[16] Reichert and Michael[34] have studied the polymerization of ethylene in a bubble column reactor and report $k_\ell a$ values which decrease at above 20 wt% solids. At 30wt% solids, the decrease amounts to roughly 20% of the low-solids limit of $k_\ell a$. According to one report,[14] the negative effect on $k_\ell a$ is considerably more pronounced for particles of large size (200-500μm) than for small particles (< 100 μm). However, other workers[11] report that particles with a bimodal distribution behave similarly to those with a unimodal distribution with the same d_p. The decrease in $k_\ell a$ is related to an increase in viscosity,[30] and $k_\ell a$ only decreases severely when the relative viscosity, μ_s/μ_ℓ, is above 5.[31,32] Since the solids are not inert but actually react with the gas, the possibility of enhancement of the mass transfer rate also exists. This was investigated by Alper et al.,[32,35] who found that for very small, reactive particles, enhancement may indeed be observed. However, enhancement is only significant when the concentration of dissolved gas is very small compared to the equilibrium concentration, that is, $M_b/M_{eq} \ll 1$, or when the reactive particles are less than 10 μm in size.[32] Thus, when predicting the *onset* of mass transfer resistance, enhancement would not affect the results. The effects of $k_\ell a$ discussed above are not easily quantified, and in this study, no explicit correction for solids was made to the correlations themselves, although the effect of solids in the slurry viscosity was considered. Industrial slurry processes employ solids concentrations of around 35%,[10] and high solids concentrations may also be attained in semibatch operation.[8] The mass transfer coefficients predicted by the correlations employed here will be less accurate above 30% solids.

Another point concerns the calculation of power per unit volume which appears in Eqs. (10) and (16). This is determined using the standard power number correlations of Rushton and co-workers,[36] with the following assumptions. For the lab reactor, the correlation for a six-bladed turbine in an unbaffled vessel was used (Figure 15-5 in Ref. 36) to obtain N_p the power number. Because data suggest that a two-bladed turbine yields roughly half the power of a six-bladed one,[37] the N_p value was halved in order to correspond better to a magnetic stir bar. This yields a seemingly reasonable

value for N_p in the turbulent region of around 0.5, which is slightly higher than the value of 0.364 employed by Brockmeier. For the pilot plant and industrial reactors, the correlation for a six-bladed turbine in a baffled vessel was used (Figure 15-6 in Ref. 36).

For sparged systems, the power for a given agitation rate is less than the power for an ungassed system, and for the prediction of gassed power the correlation due to Michel and Miller[38] (here converted to c.g.s. units),

$$\frac{P_g}{P_{ug}} = 0.2296\left(\frac{P_{ug}^2 N D_I^3}{Q^{0.56}}\right)^{0.45} \tag{18}$$

has been considered reliable. The effect of higher than atmospheric pressures should also be considered. Sridhar and Potter[21] find the effect of increased gas density to be an increase in the holdup. For example, increasing the pressure from atmospheric to around 10 atm led to an increase in holdup from 20 to 30%. In addition, the bubble diameter decreased, but d_b (in cyclohexane) still remained above the 2 mm range. These workers correlated the interfacial area by modifying Calderbank's correlation, Eq. (5), to include the total energy dissipated in the system. Their multiplicative correction to the interfacial area is given as

$$\phi_p = \frac{P}{P_g}\left(\frac{\rho_g}{\rho_a}\right)^{0.16} \tag{19}$$

where P, the total power, is given as the sum of P_g, the gassed power (as determined above), P_k, the kinetic power of the gas, and P_e, the power due to expansion of the sparged gas and ρ_a is the density of air under the conditions of the system. These workers investigated a wide range of conditions (24-150°C and 1-10 atm), in a pilot plant reactor. Hence, their correction should be applicable to the conditions considered here, and (18) will be applied to all the correlations for *sparged* reactors.

A final consideration is the minimum agitation rate required for suspension of the solids. The agitation rate at which the particles are just suspended is of paramount importance, the criteria being that no particle resides at the reactor bottom for longer that 1–2 s[2,10,11,20] This agitation rate is given by Zweiterung's relation[2]

$$N_{\text{sus}} = \left[\left(\frac{D_T}{D_I}\right)^{4/3} d_p^{0.2}\mu_\ell^{0.1} g^{0.45}(\rho_p - \rho_\ell)/\rho_\ell^{0.05} D_I^{0.85}\right](\phi_w \rho_s)^{0.13} \tag{20}$$

Here, the largest particle size which represents a significant fraction should be used for d_p.[10]

The Calculation Procedure

Having discussed the correlations and assumptions which are applicable to the system, their implementation in our gas-liquid mass transfer calculations will now be discussed. To simulate currently relevant catalysts, catalyst

activities corresponding to the following systems for polymerization of propylene were assumed:

(a) Stauffer AA with DEAC (~ 250 g/g-cat.h)
(b) Stauffer AA with TEA (~ 500 g/g-cat.h)
(c) Solvay catalyst (~ 1500 g/g-cat.h)
(d) Montedison catalyst (~ 5500 g/g-cat.h)

where the approximate yields at 7 atm and 70°C are given in parentheses.[39-41] An arbitrary catalyst activity was also considered. For the ethylene polymerization system, the diluent was chosen as hexane and the calculations were performed for 3, 5, 7, 10, and 35 atm, at 80°C. The above catalysts' activity for ethylene polymerization at 80°C was assumed to be ten times that for propylene polymerization. For propylene polymerization, the diluent is heptane and the conditions selected were 1, 5, 7, 10, and 15 atm at 30, 50, 70, and 90°C. The main problem in using the correlations for $k_\ell a$ is the determination of the requisite physical properties. In particular, it is important to distinguish between the properties of the slurry and the solution (diluent plus soluble polymer). The slurry properties reflect the presence of the solids (growing polymer particles) and are "seen" by the impeller.[33] On the other hand, the properties "seen" by the gas bubbles are considered to be the properties of the solution. Hence, in the correlations for $k_\ell a$, the properties of the slurry will be used only for determining the power per unit volume, that is, in the Reynolds and Froude numbers, but not in the Schmidt number. The solution viscosity for propylene polymerization takes into account the presence of soluble polymer. Unless otherwise noted, soluble polymer was assumed to be 10% of the total polypropylene produced. The solution viscosity is related to that of pure diluent via the Martin equation

$$\mu_\ell/\mu_d = 1 + C_{\text{sol}}[\eta]\exp(k_{\text{H}}C_{\text{sol}}[\eta]) \tag{21}$$

where $[\eta]$ is the intrinsic viscosity for soluble polymer and k_{H} is the Huggins constant. For polypropylene in heptane, reasonable values of 0.43 for $[\eta]$ and 0.63 for k_{H} were used. For polyethylene, it was not possible to estimate either these properties or the amount of soluble polymer. Hence, the pure diluent viscosity was employed in the correlations, in place of the solution viscosity. To get the slurry viscosity, Ford's equation

$$\mu_s/\mu_\ell = \frac{1 + 0.5\phi_v}{(1 - \phi_v)^2} \tag{22}$$

was used, as suggested by Brockmeier and Rogan.[8] Here, ϕ_v is the volume fraction of polymer (soluble and insoluble) in the slurry. For semibatch operation ϕ_v was calculated assuming one hour's reaction, while for continuous operation the steady state polymer concentration was assumed.

The diffusivity of monomer in the diluent liquid is another physical parameter which must be calculated. For this, the widely used Wilke-Chang correlation[42] was employed. Some caution is necessary in determining the ap-

propriate value of the viscosity to use in the correlation. Diffusion in polymer solutions is a complex topic, because the diffusivity for low-molecular weight solutes is a strong function of both temperature and polymer concentration.[43] However, it can definitely be said from the literature that use of the apparent solution viscosity in the Wilke-Chang correlation leads to serious underestimation of the diffusion coefficient.[44,45] Indeed, it has been reported that for some systems, the diffusion coefficient in polymer solutions is actually higher than in pure diluent.[44] However, most experimental data indicate that for relatively low concentrations of soluble polymer (< 10wt%), the diffusion coefficient varies by less than a factor of 2-3 from its value in pure solvent.[46] In view of these uncertainties, it was considered preferable to use the pure diluent viscosity rather than the solution viscosity in the Wilke-Chang correlation, as recommended in Ref. 45.

To calculate the equilibrium monomer concentration M_{eq}, at any gas phase condition, a program originally developed by T. W. Taylor and G. E. Mann[47] was modified to allow calculation of the vapor-liquid equilibria for ethylene and propylene in hexane or heptane. The densities and fugacity coefficients in the phases were determined by the Benedict-Webb-Rubin equation of state.[48] As recommended by Orye,[49] a mixing-rule constant M was fit to available binary data. For ethylene in heptane, M = 2 gave an excellent fit to the extensive VLE data of Kay,[50] while for ethylene in hexane, M = 1.9 gave an adequate fit for data taken at 30–100°C by Zhuze et al.[51] See *Note Added in Proof* preceding the References. The equilibrium concentrations obtained for ethylene in hexane and propylene in heptane are shown in Figures 1 and 2, respectively.

The values of the physical properties and constants used to calculate the viscosity and diffusion coefficient, or used directly in the correlations for $k_\ell a$, are listed in Table I. The dimensions of the three example reactors considered are shown in Table II. Most calculations were performed for the range of rpm 300–1000, because this is the region in which many reactors are operated, and

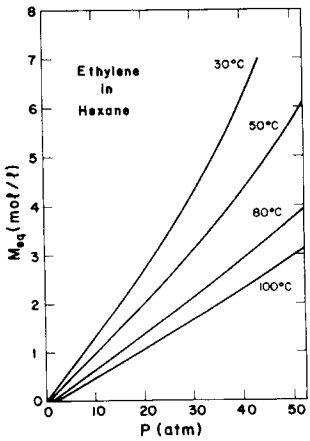

Fig. 1. Equilibrium monomer concentration of ethylene in hexane calculated using Benedict-Webb-Rubin equation of state.

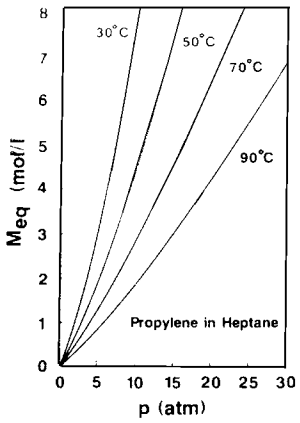

Fig. 2. Equilibrium monomer concentration of propylene in heptane calculated using Benedict-Webb-Rubin equation of state.

TABLE I
Physical Properties[57-59]

Property	Ethylene/hexane 80°C	Propylene/heptane 30°C	50°C	70°C	90°C
Diluent Density ρ_d [g/cm^3]	0.602	0.675	0.660	0.644	0.624
Diluent viscosity μ_d [c.p.]	0.184	0.365	0.296	0.252	0.216
Diluent surface σ_d tension [dyn/cm]	12.2	18.6	16.7	14.8	13.9
Molar volume at normal BP [cm^3/mol]	48.9			68.8	
Polymer density ρ_p [g/cm^3]	0.96			0.90	

Additional data: Monomer gas densities at 3, 5, 7, 10, and 35 atm and 70°C for ethylene, calculated using Ideal Gas Law. At 1, 5, 7, 10 and 15 atm and 30, 50, 70, and 90°C for propylene, obtained from Ref. 58.

also because there are doubts as to the validity of any of the correlations at very low agitation rates.[12,53]

RESULTS

Because gas-liquid mass transfer is very different in sparged and unsparged systems, these will be considered separately. Laboratory and pilot-scale reac-

TABLE II
Reactor Dimensions

[cm]	D_T	D_I	H	D_I/D_T
Lab (200 mL)	7.0	2.33	5.2	1/3
Pilot (1/2 gal)	12.5	4.17	15.4	1/3
Industrial	458	91.6	458	1/5

A sparger orifice diameter of 5 mm was assumed for the pilot reactor.

tors in which kinetic studies are performed are frequently unsparged reactors in which monomer gas is introduced over the agitated diluent. Industrial reactors may be sparged, unsparged, or may introduce monomer as a liquid. In the latter case, the problem of gas-liquid mass transfer is circumvented.

Unsparged Systems

To insure that the mass transfer correlations chosen are consistent with available data, comparisons with literature data for olefin polymerization were sought. Several workers have detected gas-liquid mass transfer resistence, but detailed results are only available for a handful fo systems. In fact, the only complete data of polymerization rate against rpm were provided by Böhm.[54] The results of simulation of the gas-liquid mass transfer resistance for his catalyst using Lamont and Scott's correlation are shown accompanied by his data in Figure 3. Considering the reliability of the original correlation and the number of assumptions made, the agreement is surprisingly good. In fact, as subsequent figures will illustrate, it is not uncommon to have a residual mass transfer resistance of 5–10% even at the high stir rates employed by Böhm. While other workers do not show an explicit relationship between rpm and catalyst loading, the loading at which mass transfer re-

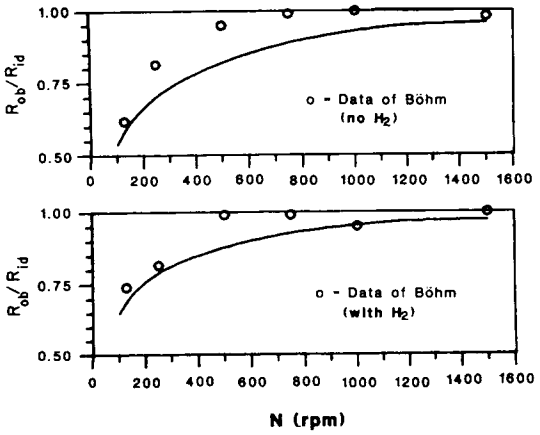

Fig. 3. Comparison of correlation of Lamont and Scott for unsparged reactors with experimental data of Böhm for ethylene polymerization in hexane.[54] Catalyst activity: 3800 g/g-cat.h (no hydrogen), 2400 g/g-cat.h (with hydrogen). Catalyst loading = 0.0235 g-cat/L.

sistence becomes significant was indicated for catalysts of known activity by Keii,[4] and Berger and Grieveson.[55] Berger and Grieveson[55] employed a reactor with a vibrating stirrer for the polymerization of ethylene at 40°C, using loadings of 0.15 and 0.9 g-cat/L. They found considerable diffusion resistance at the high loading, with the activity decreasing by a factor of two when the amplitude of the vibrator was reduced. Correcting their catalyst activity and simulating for a comparable situation (propylene polymerization in a pilot plant at 50°C), it was found that around 7% mass transfer resistance would be anitcipated at the low loading at 200 rpm, while at the high loading the mass transfer resistance would be around 30% at 200 rpm decreasing to 6% at 1000 rpm. Keii et al.[4] varied the agitation rate in propylene polymerization with a decaying catalyst at 41°C, employing catalyst loadings of 1 and 4 g-cat/L. Again, at the high loading gas-liquid mass transfer effects were detected. The observed rate was markedly lowered when the agitaiton rate was reduced to 250 rpm. Simulating for their catalyst near the beginning of polymerization showed that around 10% mass transfer resistance would be anticipated at the low loading at 250 rpm, while at the high loading the mass transfer resistance would be around 50% at 250 rpm decreasing to around 16% at 1000 rpm. Thus, in both of these cases, the simulations seem to be quite consistent with the actual observations, when the correlation of Lamont and Scott (15) with correction for vortex area (16) was employed. This is in contrast to the Calderbank correlation (14), which overestimated the gas-liquid mass transfer resistence.

Having confirmed the applicability of Lamont and Scott's correlation for unsparged systems, some calculations of gas-liquid mass transfer resistance based on the observed rate of polymerization are presented next. Some results for ethylene polymerization are shown in Figures 4 and 5, while Figures 6 and 7 are for propylene polymerization. Note that the observed rates, R_{vob}, would in principle depend on the intrinsic catalyst activity and the catalyst loading. Thus the indicated values of R_{vob} could be obtained for any catalyst. Figures 5 and 7 are calculated for lower reaction rates, to permit accurate determina-

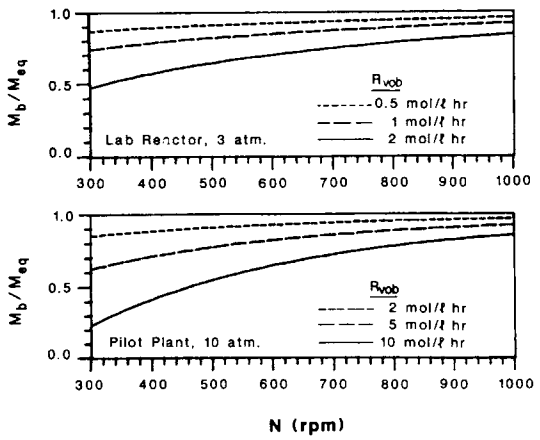

Fig. 4. Gas-liquid mass transfer resistance in ethylene polymerization at various observed polymerization rates. Lab reactor (3 atm) and pilot plant reactor (10 atm). Temp = 80°C.

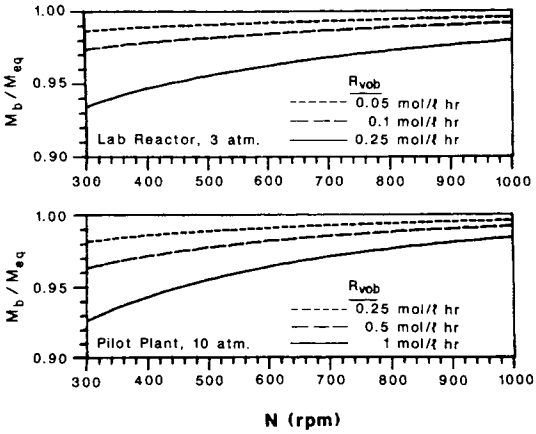

Fig. 5. Gas-liquid mass transfer resistance in ethylene polymerization at various observed polymerization rates. Lab reactor (3 atm) and pilot plant reactor (10 atm). Temp = 80°C.

tion of the catalyst loadings at low levels of mass transfer resistence. For ethylene polymerization, one sees that the mass transfer resistance becomes significant at above a volumetric mass transfer rate of around 0.25 mol/L.h, for the lab reactor, or around 1 mol/L.h, for the pilot plant at 10 atm. (Here, "significant" is taken to mean greater than 5% for some agitation rates commonly employed.) For propylene polymerization, mass transfer resistance becomes important at approximately 0.5 mol/L.h for a lab reactor at 1 atm and 5 mol/L.h for a pilot plant at 15 atm. In general, the gas-liquid mass transfer resistance is more severe for ethylene polymerization than for propylene polymerization, at the same temperature and pressure. Although the $k_\ell a$ values in these systems are very similar, the difference arises due to the lower equilibrium monomer concentrations for ethylene, as evident from Figure 1 and Eq. (2). To determine a suitable loading for any type of catalyst, the researcher should first choose from the figures an acceptable level of mass

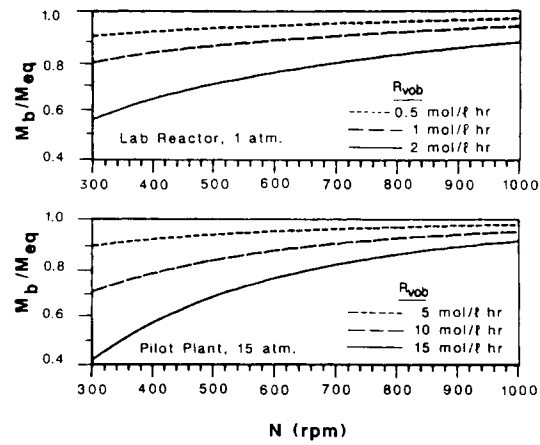

Fig. 6. Gas-liquid mass transfer resistance in propylene polymerization at various observed polymerization rates. Lab reactor (1 atm) and pilot plant reactor (15 atm). Temp = 70°C.

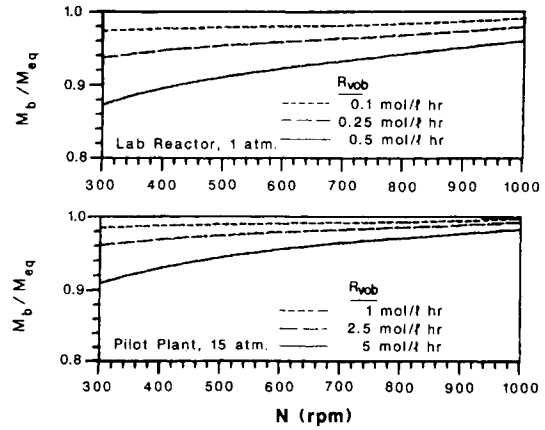

Fig. 7. Gas-liquid mass transfer resistance in propylene polymerization at various observed polymerization rates. Lab reactor (1 atm) and pilot plant reactor (15 atm). Temp = 70°C.

transfer resistance, corresponding to a given volumetric mass transfer rate R_{vob} [mol/L.h]. Knowing the ideal catalyst productivity at the pressure in the figure, R_{id} [g/g-cat/h], as defined in Eq. (4), and recalling the definition of R_{vob} from Eq. (3), then

$$R_{vob} = R_{id}\left(\frac{M_b}{M_{eq}}\right)\frac{W}{MW} \tag{23}$$

the proper catalyst loading, W [g-cat/L] is given by

$$W = \frac{R_{vob}(MW)}{R_{id}\left(\dfrac{M_b}{M_{eq}}\right)} \tag{24}$$

where M_b/M_{eq} is the level of mass transfer resistance that can be tolerated. This loading is relatively insensitive to pressure changes, because the polymerization rates and the monomer concentrations are both roughly proportional to the pressure. Thus, for a given reactor type, the loading determined can be used over the full range of operation. We illustrate with an example.

Example 1. A catalyst for propylene polymerization produced 200 g/g-cat in a one-hour reaction in a laboratory glass bottle reactor at 70°C and atmospheric pressure. The catalyst loading was 0.03 g-cat/L and the stirring rate was 500 rpm. Let us calculate the loading for this catalyst in a pilot plant at 70°C and 15 atm, at the same stirring rate, where it is desired that $M_b/M_{eq} > 0.95$.

First, check for mass transfer resistance at the original laboratory conditions. At 1 atm and 70°C the catalyst productivity was found to be

$$R_{ob} = 200\ g/g\text{-}cat.h.$$

With a loading of 0.03 g-cat/L, the observed average volumetric rate is

$$R_{vob} = R_{ob}W/MW = \frac{200 \times 0.03}{42} = 0.143\ \text{mol/L.h}$$

From Figure 7 (top) we see that there is less than a 4% rate reduction due to gas-liquid mass transfer resistance. Hence $R_{ob} \sim R_{id}$ for the lab reactor. To scale up the pilot-plant reactor at the higher pressure, we note from Figure 2 that the equilibrium monomer concentrations at 70°C and 1 and 15 atm are 0.162 and 4.54 mol/L, respectively. Thus, the ideal catalyst productivity at 15 atm is

$$R_{id} = 200 \times \frac{4.54}{0.162} = 5605 \text{ g/g-cat.h}$$

From Figure 7 (bottom) for $M_b/M_{eq} > 0.95$ at 500 rpm, $R_{vob} \cong 3$ mol/L.h is the critical observed rate. Using Eq. (24), we obtain the maximum loading for less than 5% gas-liquid mass transfer rate reduction as

$$W = \frac{3(42)}{(5605)(0.95)} = 0.024 \text{ g-cat/L}$$

In this case, the loading used in the laboratory reactor must be decreased by ~ 20% for the pilot plant. This example also illustrates that in selecting a catalyst loading, a compromise between high reaction rate and the tolerable mass transfer resistance must usually be reached. To make the mass transfer resistance truly negligible, one would have to use very small amounts of catalyst. Thus, under normal operating conditions where high productivity is desired, it will not be uncommon to have a mass transfer resistance of 5–10%, that is, $M_b/M_{eq} = 0.90$–0.95, in agreement with the conclusion reached by Brockmeier and Rogan.[8]

Example 2. The second example will illustrate that assuming that the same loading will be valid on scaleup can sometimes be dangerous. We consider a new high activity catalyst for propylene polymerization which is currently being tested in an atmospheric pressure lab reactor at 50°C and 500 rpm. The catalyst activity was 240 g/g-cat.h under these conditions. It is desired to scale up to a pilot-plant reactor operating at 15 atm, 500 rpm, and 90°C to gain kinetic and polymer property data. In the lab reactor, the current loading of 0.03 g-cat/L indicates an observed volumetric reaction rate of

$$R_{vob} = 240 \times 0.03/42 = 0.17 \text{ mol/L.h}$$

Assuming the observed rate is equal to the ideal rate, Figure 7 shows that at the agitation rate of 500 rpm $M_b/M_{eq} > 0.95$ at 70°C. At 50°C, there will be less mass transfer resistance. However, for the pilot plant at 90°C ($M_b = 3.1$ mol/L), the catalyst activity would be ~ 18250 g/g-cat.h, assuming an activation energy of 12 kcal/mol. Then, at the same loading, the ideal volumetric rate would be

$$R_{vid} = 18250 \times 0.03/42 = 13.0 \text{ mol/L.h}$$

and from Figure 6 (bottom), there would be a very significant mass transfer resistance. The program calculations indicate that the mass transfer resistance would be over 50% at 300 rpm, and around 10% even at 1000 rpm. This is

clearly unacceptable for kinetic studies. Since we are limited to 1000 rpm in this particular pilot plant, we must go to a lower loading. For a loading of 0.006 g-cat/L, the ideal rate would be ~ 2.6 mol/L.h, and from Figure 7 (bottom) this appears to be a safe loading. Detailed calculations for 90°C indicate that there is actually less than 4% mass transfer resistance at 500 rpm with this reduced catalyst loading. The difference between this example and the previous one is the change in temperature between the reactors, leading to an increase in intrinsic rate by a factor of 7.8 between 50 and 90°C. Clearly, in this common situation, the assumption that the same catalyst loading may be employed is very poor. The effect of temperature on gas-liquid mass transfer will be discussed in more detail below.

One of the most important reactor variables is the temperature. Sometimes polymerizations in the lab are carried out at relatively low temperatures of 30–50°C, but most pilot work is done at or near the temperatures in industrial reactors, e.g., 60–90°C. The effect of temperature on gas-liquid mass transfer was calculated for propylene polymerization at a constant observed rate (R_{vob}). The results are illustrated in Figure 8 for a lab reactor at 1 atm, and Figure 9 for a pilot plant at 7 atm. In both cases, $k_\ell a$ increase as the temperature is raised, but this increase is offset by a decrease in solubility of the monomer (see Fig. 2), so that gas-liquid mass transfer resistence is actually more severe at the higher temperatures even when there is no change in reaction rate with temperature. Hence, Figures 4–7 will be conservative for low polymerization temperatures, but for propylene polymerization at temperatures significantly higher than 70°C or ethylene polymerization at temperatures significantly higher than 80°C, these figures will underestimate the mass transfer resistance.

In the lab reactor, the $k_\ell a$ values range from around 0.005 s^{-1} at 300 rpm to 0.02 s^{-1} at 1000 rpm (Fig. 8). In the pilot plant, the corresponding values are 0.002–0.015 s^{-1} (Fig. 9), and for an industrial reactor with a 40% solids loading, the values range from 4×10^{-4} to 2×10^{-3} s^{-1} (Fig. 10). The trend toward smaller $k_\ell a$ values as the reactor size increases is illustrated more

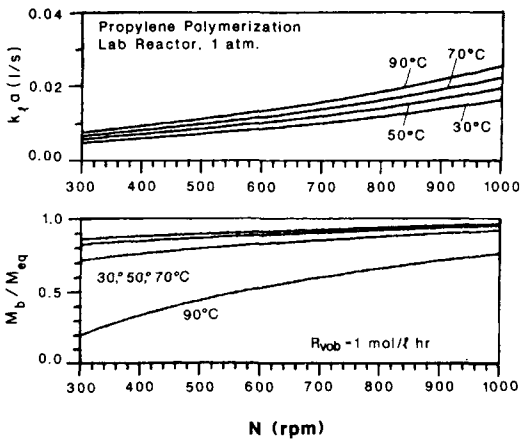

Fig. 8. Effect of temperature on gas-liquid mass transfer resistance. Propylene polymerization in lab reactor at 1 atm pressure. Observed rate of polymerization R_{vob} = 1 mol/L.h.

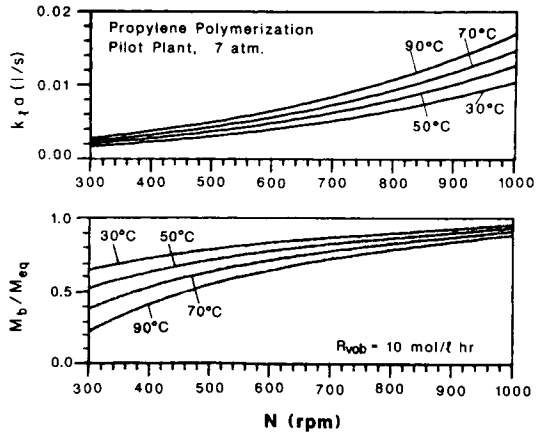

Fig. 9. Effect of the temperature on gas-liquid mass transfer reisitance. Propylene polymerization in pilot plant reactor at 7 atm pressure. Observed rate of polymerization R_{vob} = 10 mol/L.h.

clearly in Figure 11, for a polymerization with a Solvay-type catalyst at 5 atm and 70°C. The decrease in $k_\ell a$ as reactor size increases (in the absence of sparging) is due to the fact that the free surface per unit volume ($a = A/V$) is roughly proportional to $1/H$. The increase in power per unit volume required to maintain the same agitation rate, shown in Figure 12, is insufficient to offset this decrease in A/V as the reactor becomes larger. While the power consumption is not significant for lab or pilot-plant reactors, it can easily reach an order of 100 kW/m^3 for industrial reactors (Fig. 12). Hence, the high rpm's which are commonly employed at the pilot stage may be prohibited in the industrial case. This is, of course, because of the large impeller diameter for the industrial reactor (P/V is proportional to $N^3D_I^5$ in the turbulent region, where N_p is constant). However, the impeller diameter cannot be made very small, because this may result in imperfect solids suspension, a highly undesirable condition. The design of a large reactor should attempt to maxi-

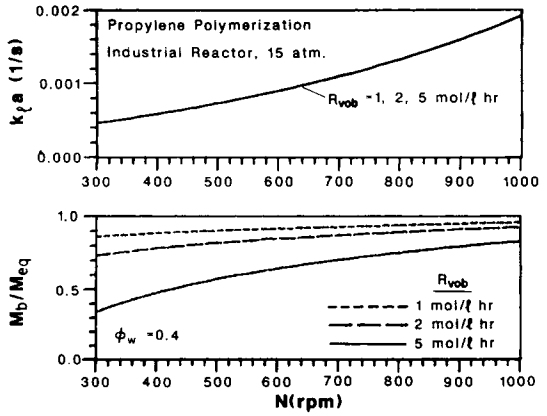

Fig. 10. Gas-liquid mass transfer resistance in an industrial reactor. Propylene slurry polymerization at observed polymerization rates, solids loading = 40 wt%.

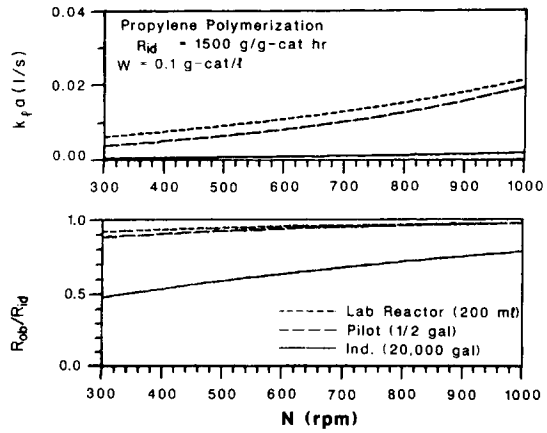

Fig. 11. Comparison of gas-liquid mass transfer resistance in laboratory, pilot plant and industrial reactors for propylene slurry polymerization. Lab reactor, pilot plant, and industrial reactors at 5 atm. Intrinsic polymerization rate R_{vid} = 3.57 mol/L.h.

mize surface aeration, for instance by locating an additional impeller near the liquid surface,[13,33,53] and by having H/D_T relatively small. A self-inducing impeller might also be used.[17] If this still results in inadequate transfer rates, it may be necessary to employ a more effective method of introducing monomer to the reactor. This can be accomplished by sparging (see next section), or by liquifying the monomer and dispersing it as liquid.

While these qualitative trends for the industrial reactor are considered correct, the calculated mass transfer resistance is probably not as accurate as that for the smaller reactors. This is because industrial reactors routinely operate at a higher solids loading of around $\phi_w = 0.4$ (against $\phi_w < 0.25$ for lab and pilot scale) when the catalyst loading is suitably low. In this region, the slurry is likely to behave as a non-Newtonian fluid,[56] and the mass transfer correlations may not be truly applicable. As mentioned earlier, high solids concentrations are expected to reduce the value of $k_\ell a$ considerably,

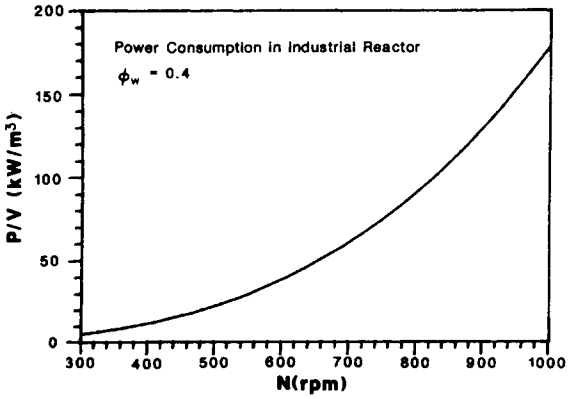

Fig. 12. Power consumption in industrial reactor for propylene slurry polymerization at a solids content of 40 wt%.

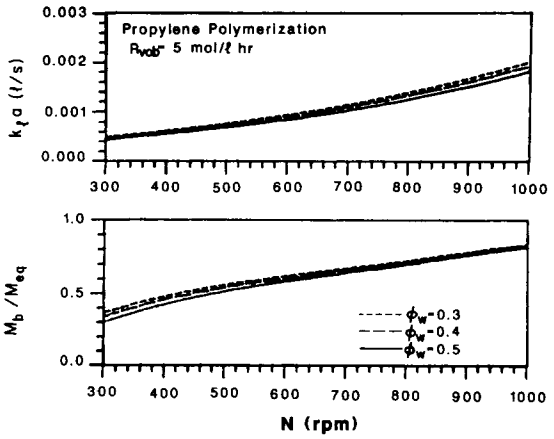

Fig. 13. Gas-liquid mass transfer resistance in propylene polymerization in an industrial reactor at various solids contents. Observed rate of polymerization R_{vob} = 5 mol/L.h.

but as shown in Figure 13, this effect is not predicted adequately with the correlations used here. The effect of high solids concentrations on $k_\ell a$ should also be kept in mind when long polymerization times are employed in laboratory reactors or pilot plants.

Although the calculations for observed polymerization rate, presented in Figures 4–7, should be most useful to researchers in predicting the "safe" loading regime for their catalysts, some calculations for specific catalyst systems were also performed. For Stauffer AA type catalyst with DEAC[39] as cocatalyst for propylene polymerization in a lab reactor at 70°C (R_{id} ~ 150 g/g-cat.h), as employed by Yuan et al.[7] and Brockmeier and Rogan,[8] the catalyst may be loaded up to around 0.5 g-cat/L (Fig. 14). For Solvay catalyst[40] in a pilot plant operating at around 7 atm and 70°C (R_{id} ~ 1500 g/g-cat.h) the loading should be less than about 0.05 g-cat/L for less than 5% mass transfer resistance at 500 rpm (Fig. 15), and for Montedison catalyst[41]

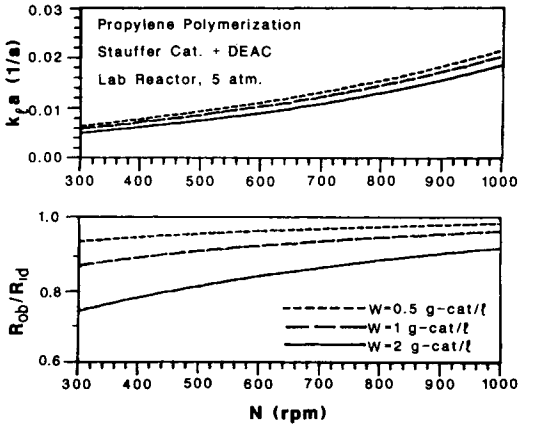

Fig. 14. Gas-liquid mass transfer resistance for propylene polymerization over Stauffer catalyst[39] with diethylaluminum chloride cocatalyst at various catalyst loadings. Lab reactor at 5 atm.

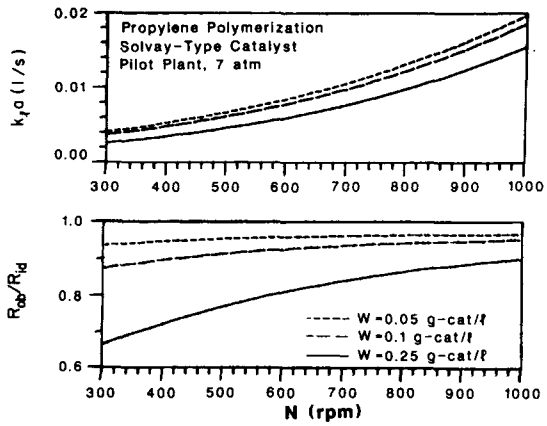

Fig. 15. Gas-liquid mass transfer resistance for propylene polymerization over Solvay-type catalyst[40] at various catalyst loadings. Pilot plant reactor at 7 atm.

(R_{id} ~ 5500 g/g-cat.h) in a pilot plant at 7 atm and 70°C, the critical loading is around 0.015 g-cat/L (Fig. 16). As mentioned above, the operating pressure has a relatively small effect on these results, but the safe loading is strongly affected by the temperature because of the activation energy for polymerization and the reduced monomer solubility at higher temperatures. This effect is illustrated for the Montedison catalyst in Figure 17, with an assumed activation energy of 15 kcal/mol. The loading of 0.05 g-cat/L is tolerable at 30–50°C, but at higher temperatures, gas-liquid mass transfer resistance becomes severe. The amount of soluble polymer can also have a major influence on $k_\ell a$, and hence the gas-liquid mass transfer resistance. All of the preceding calculations were made assuming 10% soluble polymer for propylene polymerization and no solubles for ethylene polymerization. This is considered reasonable, since most catalysts of industrial interest today produce very small amounts of soluble polymer. However, for larger amounts of soluble polymer the mass transfer effects can be significant. This is illustrated in Figure 18 for Stauffer AA catalyst with tetraethylene ammonium (TEA) as

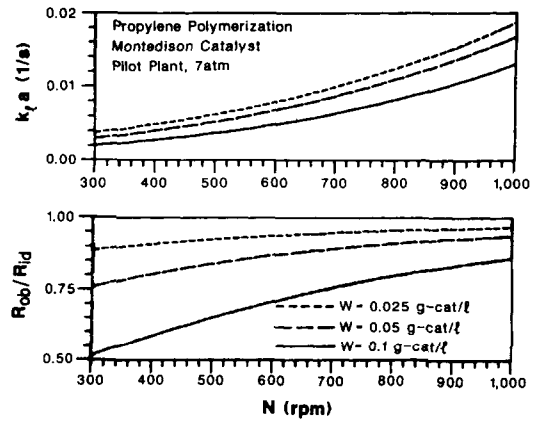

Fig. 16. Gas-liquid mass transfer resistance for[41] propylene polymerization over Montedison-type catalyst at various catalyst loadings. Pilot plant reactor at 7 atm.

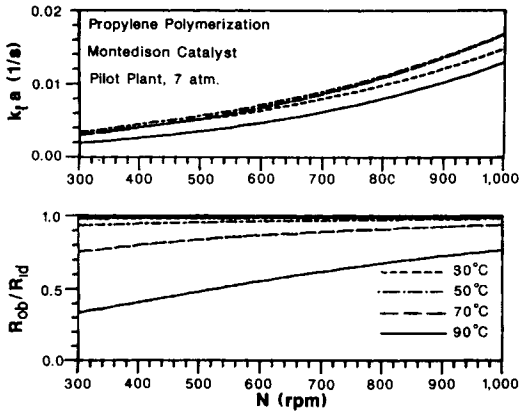

Fig. 17. Effect of temperature on gas-liquid mass transfer resistance in propylene polymerization over Montedison-type catalyst.[41] Catalyst loading = 0.05 g-cat/L. Pilot plant reactor at 7 atm and various temperatures.

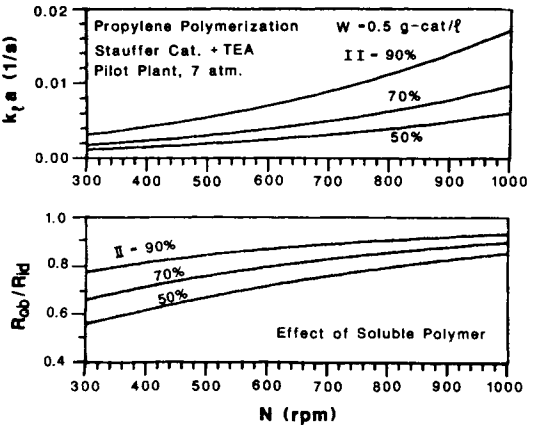

Fig. 18. Effect of soluble polymer on gas-liquid mass transfer resistance in propylene polymerization over Stauffer catalyst[39] with triethylaluminum as cocatalyst. Catalyst loading = 0.5 g-cat/L, pilot plant reactor at 7 atm.

cocatalyst, a system which does in fact produce rather large amounts of atactic material.[39] A variation in isotactic index (II) from 90 to 50% can result in a decrease in $k_\ell a$ by an order of magnitude, so that the gas-liquid mass transfer resistence becomes severe.

Sparged Systems

In contrast to unsparged systems, there is no data available for direct comparison for sparged stirred reactors. In the absence of such data, the three correlations for $k_\ell a$ for sparged systems [Eqs. (6)–(11)] were compared, as an indication of their usefulness. The results are illustrated for a ges recycle ratio of R = 2 in Figure 19, and for R = 10 in Figure 20, for a situation which is mass transfer limited. These recycle ratios correspond to superficial gas velocities of 0.30 cm/s and 1.26 cm/s, respectively, which fall within the range

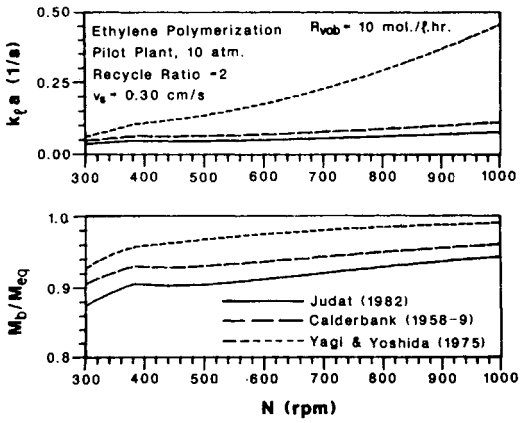

Fig. 19. Gas-liquid mass transfer resistance in polymerization of ethylene in a sparged pilot plant reactor. Comparison of correlations of Yagi and Yoshida, Calderbank and Judat for $k_\ell a$. Observed rate of polymerization R_{vob} = 10 mol/L.h, monomer recycle ratio = 2, superficial gas velocity = 0.30 cm/s.

that has commonly been studied.[18,21b] From these figures it may be seen that there is generally better agreement between the correlations for $k_\ell a$ at low rpm. Note that, Judat's correlation[18] is the most conservative, while Yagi and Yoshida's correlation[16] is the least conservative. Since Judat's correlation is the most recent and incorporates the greatest amount of data (including the data of Calderbank), it may be considered the most reliable. Hence, we shall use Judat's correlation for our analysis.

It was noted above that unsparged reactors of industrial size are most likely to suffer from gas-liquid mass transfer resistance. In the case of ethylene polymerization, the monomer is not readily liquified, and hence sparging might be the method of choice for increasing the interfacial area in industrial slurry systems. For this reason, all the calculations for sparged reactors were

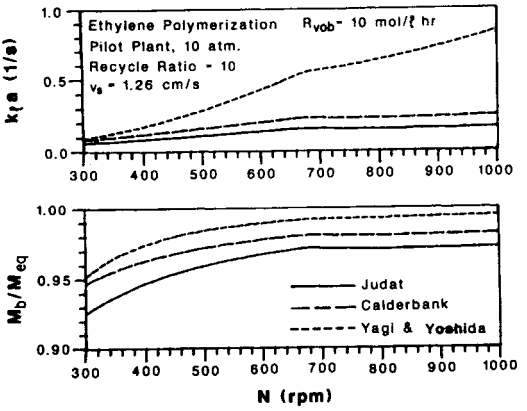

Fig. 20. Gas-liquid mass transfer resistance in polymerization of ethylene in a sparged pilot plant reactor. Comparison of correlations of Yagi and Yoshida, Calderbank and Judat for $k_\ell a$. Observed rate of polymerization R_{vob} = 10 mol/L.h, monomer recycle ratio = 10, superficial gas velocity = 1.26 cm/s.

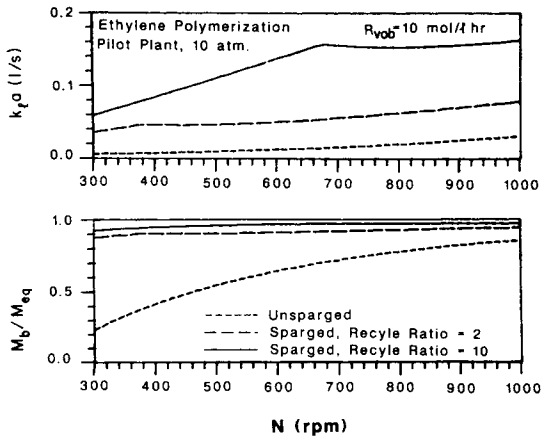

Fig. 21. Gas-liquid mass transfer resistance in polymerization of ethylene. Effect of sparging. Pilot plant reactor at 10 atm. Observed rate of polymerization R_{vob} = 10 mol/L.h. Correlation of Judat was used for sparged reactors, correlation of Lamont and Scott was used for unsparged reactors.

performed for ethylene polymerization, despite a lack of knowledge about the amount of soluble polymer in the ethylene polymerization system. Figure 21 illustrates that sparging is capable of increasing $k_\ell a$ by about an order of magnitude. Thus, sparging may practically eliminate the gas-liquid mass transfer resistance at close to critical loadings, as shown experimentally for polymerization in a bubble column by Reichert and Michael.[34] These authors found $k_\ell a$ values from 0.01 s^{-1} at low superficial gas velocities (v_s = 1 cm/s), increasing to around 0.08 s at v_s = 9 cm/s. Figure 21 shows that for both sparging and agitation, with 300 rpm agitation, $k_\ell a$ is approximately 0.065[1] and with 1000 rpm agitation, $k_\ell a$ = 0.15 s^{-1} for u = 1.26 cm/s. This comparison indicates that introduction of sparged gas alone is considerably less effective than sparging coupled with agitation. Of course, the benefit of sparging must be weighed against the increased power requirement and system complexity demanded. Note also, from Figure 21 that significant benefits may be realized at very moderate sparge rates (e.g. v_s = 0.30 cm/s for R = 2).

Solids Suspension

In the design of slurry reactors, the minimum agitation rate for solids suspension is of primary interest.[3] This minimum agitation rate, determined by Eq. (20) based on a polymer particle size of 200 μm, generally ranged from 300 to 450 rpm for lab and pilot-plant reactors. In this range of agitation rates, it is anticipated that the solid phase will be poorly suspended, which in turn may result in serious inhomogeneity in the liquid. Gas-liquid mass transfer would surely be adversely affected. This effect may explain some data, reported by Keii et al.,[4] showing a very large initial loss in polymerization rate when agitation was reduced to values in this range. From the point of view of both gas-liquid and solid-liquid mass transfer, agitation rates of less than around 500 rpm are therefore considered inadvisable for kinetic studies.

Sufficient agitation rates are especially crucial when the solution viscostiy increases substantially as the reaction proceeds. For relatively low solids concentrations, such as are observed for low reaction rates in semibatch systems, both the solution and slurry viscosities are less than 1 c.p., but as the solids concentration is increased, the calculated viscosities increase by an order of magnitude or more. A lowering of the tacticity from 90% to 70% can also result in an order-of-magnitude increase in the viscosities, to values of around 30 c.p. for the slurry viscosity. Chinese workers Furui et al.[55] report viscosities of the order of 100 c.p. for a polypropylene slurry with $\phi_w > 34$ wt%.

Copolymerization

Having treated gas-liquid mass transfer for homopolymerization of ethylene and propylene at length, some brief remarks will be made on copolymerization. In liquid-phase copolymerization with a mixed monomer stream, the monomer incorporation, and hence the copolymer properties, will depend on the relative concentrations of the monomers in the diluent. For this reason, it is extremely important to know both the equilibrium concentrations and whether gas-liquid mass transfer resistence is present. Table III illustrates the calculated ratios of propylene to ethylene in the *gas phase* at various pressures, for specified mole ratios of the components in the *liquid phase* (heptane). The calculations were performed for $M_{bP}/M_{bE} = 0.5$, 1, 4, and 10

TABLE III
Gas Phase Compositions for Copolymerization of Ethylene and Propylene in Heptane[a]

T = 70°C						
			$M_{bP}/M_{bE} = 4$			
P (atm)	2.1	4.8	9.4	19.6	25.1	30.7
M_{bP} (mol/L)	0.26	0.68	1.43	3.23	4.31	5.54
Y_P/Y_E	1.27	1.29	1.33	1.44	1.52	1.64
			$M_{bP}/M_{bE} = 1$			
P (atm)	2.4	5.5	11.0	16.9	23.1	36.6
M_{bP} (mol/L)	0.13	0.34	0.71	1.11	1.56	2.61
Y_P/Y_E	0.32	0.32	0.33	0.35	0.36	0.40
			$M_{bP}/M_{bE} = 0.5$			
P (atm)	2.2	4.9	9.6	20.0	31.6	
M_{bP} (mol/L)	0.065	0.17	0.35	0.74	1.21	
Y_P/Y_E	0.159	0.161	0.165	0.175	0.190	
			$M_{bP}/M_{bE} = 10$			
P (atm)	1.97	3.6	10.5	18.0	21.9	
M_{bP} (mol/L)	0.33	0.67	2.22	4.11	5.22	
Y_P/Y_E	3.19	3.22	3.38	3.61	3.78	
P = 10 atm			$M_{bP}/M_{bE} = 1$			
T (°C)	30	50	70	90		
M_{bP} (mol/L)	1.16	0.84	0.64	0.49		
Y_P/Y_E	0.260	0.297	0.332	0.367		

[a] Calculated by Benedict-Webb-Rubin equation of state.

at 70°C and $M_{bP}/M_{bE} = 1$ at 50°C, using the previously described vapor-liquid equilibrium program. From the table, it can be remarked that as the pressure or temperature is increased, the mole fraction of propylene in the gas phase required to maintain a constant ratio of propylene to ethylene in the liquid increases. However, as an approximation, an equimolar gas phase mixture of ethylene and propylene will be in equilibrium with a liquid phase with M_{bP}/M_{bE} around 3, for typical conditions of polymerization. To obtain a liquid phase with M_{bP}/M_{bE} around 1, the ratio of ethylene to propylene in the gas feed ranges from 2.5 to 3. If it is desired to have $M_{bP}/M_{bE} = 0.5$, the ratio of ethylene to propylene must be as high as 6. To obtain $M_{bP}/M_{bE} = 10$, on the other hand, the ratio of porpylene to ethylene in the gas needs to be only 3 to 4. The above findings can be roughly summarized by the statement that the ratio of the Henry's law coefficient ($H = M_{eq}/p$) of propylene to that of ethylene is around 3 under normal polymerization conditions. By calculations with the vapor-liquid equilibrium program, it was found that to obtain a rough estimate of the dissolved monomer concentrations in equilibrium with a gas mixture it is a good approximation (to within 15%) to use the partial pressures of each component in a Henry's law expression

$$M_{eq_i} = H_i p_i \tag{25}$$

Because mass transfer resistance affects the monomer incorporation, gas-liquid mass transfer resistance for one component is not always harmful, in contrast to the case of homopolymerization. In order to estimate the extent of gas-liquid mass transfer resistance, one may use Figures 4–7 with the observed reaction rate for each component. As pointed out above, the gas-liquid mass transfer resistance is relatively insensitive to pressure variations, so this technique is quite acceptable. If greater incorporation of the monomer which is undergoing mass transfer limitations is desired. the fraction of that monomer in the gas phase should be increased. Although the system would still be mass transfer limited, the incorporation ratio would change with the ratio of liquid phase concentrations. Alternatively, the agitation rate may be increased or the catalyst loading reduced to influence copolymer composition.

CONCLUSIONS

Correlations for the volumetric mass transfer coefficient ($k_\ell a$) were incorporated into a program which computes the gas-liquid mass transfer resistence in olefin polymerization systems. Only Lamont and Scott's correlation[25] for unsparged systems was able to be tested against experimental data, but this correlation gave satisfactory results. By this correlation, mass transfer resistance in laboratory or pilot-plant reactors may be predicted with reasonable confidence. The results should be of use to researchers in determining loadings for catalysts of a given activity level.

The present study indicates that *some* gas-liquid mass transfer resistance will exist in all laboratory, pilot scale and industrial reactors. The results presented in Figures 4–7 should be most useful in estimating these effects in laboratory and pilot scale reactors. However, for industrial reactors, uncer-

tainties about the physical properties of the high solids concentration slurry and the applicability of the correlations derived for two-phase systems mean that more detailed studies may be necessary. However, for design of industrial slurry reactors, the following rule should be kept in mind: at relatively low levels of gas-liquid mass transfer resistance, reactor scaleup is straightforward, but when gas-liquid mass transfer limiting conditions are encountered, $k_\ell a$ must be maintained sufficiently high during scaleup.[3] For polymerization of olefins, agitation rates of less than 500 rpm are not recommended in laboratory or pilot-plant work. For industrial propylene polymerization reactors, the low $k_\ell a$ values which exist make the introduction of the monomer as a liquid attractive. For ethylene polymerization reactors, sparging of monomer can greatly improve gas-liquid mass transfer. It is recommended to use the correlation of Judat to predice $k_\ell a$ in sparged systems. Finally, in copolymerization, data have been presented for gas phase concentration as a function of liquid molar ratio. As a rough approximation, the ratio of the Henry's law coefficient ($H = M_{eq}/p$) of propylene to that of ethylene is around 3. The same methodology used for determining gas-liquid mass transfer resistance for homopolymerization can be extended to liquid-phase copolymerization, using the figures in the paper as a first approximation.

APPENDIX

List of Symbols*

a	Interfacial area per unit volume [cm^2/cm^3]
A	Interfacial area in reactor [cm^2]
C_{sol}	Concentration of soluble polymer [g/dL]
d_b	Mean bubble diameter [cm]
D_I	Impeller diameter [cm]
d_p	Mean polymer particle diameter [cm]
D_T	Tank diameter [cm]
Fr	Froude Number = N^2D/g
g	Acceleration due to gravity [cm/s^2]
H	Height of liquid in reactor [cm]
H_v	Height of vortex [cm]
k_{cat}	Observed catalyst activity [L/g-cat.h]
k_ℓ	Liquid-side mass transfer coefficient [cm/s]
M	Monomer concentration [mol/L]
MW	Molecular weight of monomer
N	Agitation rate [rps]
N_P	Power number = $P_{ug}g/\rho N^3D^5$
p	Pressure [atm]
P	Total power [erg/s]
P_g	Gassed power [erg/s]
P_{ug}	Ungassed power [erg/s]
Q	Gas flowrate [cm^3/s]
Re	Reynolds Number = $\rho ND^2/\mu$

*Symbols defined and used only once in the text do not appear.

R_{vid}, R_{id}	Rates of polymerization in absence of gas-liquid mass transfer limitations [mol/L.h] and [g-poly/g-cat.h]
R_{vob}, R_{ob}	Observed rates of polymerization [mol/L.h] and [g-poly/g-cat.h]
Sc	Schmidt Number = ν/D_ℓ
V	Volume of reactor [cm^3]
v_s	Superficial gas velocity [cm/s]
W	Catalyst loading [g-cat/L]
y	Mol fraction monomer in gas phase [−]
D	Diffusivity of monomer [cm^2/s]
μ	Viscosity [g/cm.s]
ρ	Density [g/cm^3]
ν	Kinematic viscosity [cm^2/s]
σ	Surface tension [dyn/cm]
ϕ_w	Weight fraction polymer in slurry [−]
ϕ_v	Volume fraction polymer in slyrry [−]

Subscripts

d	Diluent
E	Ethylene
eq	Equilibrium
g	Gas
ℓ	Liquid
p	Polymer
P	Propylene
s	Slurry

This research was supported by the National Science Foundation and by the industrial sponsors of the University of Wisconsin Polymerization Reaction Engineering Laboratory. We are grateful to Dr. Norman F. Brockmeier of Amoco Chemical Co. for helpful comments and suggestions.

Note Added in Proof:

For propylene in heptane three sources of data were found: Fujii [52], Frank [60], and Konobeev and Lyapin [61]. The data of Fujii were fit best with $M = 2.2$, while the data from the other sources were fit best with $M = 2.0$. Comparing the ethylene in heptane data from [52] and [61] to the data of Kay [50] revealed that Fujii's data were less reliable; the data of Lyapin and Konobeev were in good agreement with Kay's data. Thus the propylene heptane data were fit with $M = 2.0$. Propylene hexane data from [61] were also fit best with $M = 2.0$.

References

1. N. F. Brockmeier, Latest commercial technology for propylene polymerization, in *Transition Metal Catalyzed Polymerizations*, Ed. by R. P. Quirk, Harwood Academic Publishers, NY, 1983.

2. R. V. Chaudhari and P. A. Ramachandran, *AIChE J*, **26** (12), 177 (1980).

3. H. Hofmann, in *Mass Transfer with Chemical Reaction in Multiphase Systems*, Vol. III, Ed. by Erdogan Alper, NATO ASI Ser., Martinus Nijhoff, The Hague, 1983.

4. T. Keii, E. Suzuki, M. Tamura, M. Murata, and Y. Doi, *Makromol. Chem.*, **183**, 2285 (1982).
5. M. N. Berger, G. Boocock, and R. N. Haward, *Adv. Catal.*, **19**, 211 (1969).
6. D. G. Boucher, I. W. Parsons, and R. N. Haward, *Makromol. Chem.*, **175**, 3461 (1974).
7. H. G. Yuan, T. W. Taylor, K. Y. Choi, and W. H. Ray, *J. Appl. Polym. Sci.*, **27**, 1691 (1982).
8. N. F. Brockmeier and J. B. Rogan, *AIChE Symp. Ser.*, **72**, (160) 28 (1976).
9. K. Van't Riet, *Ind. Eng. Chem. Proc. Des. Dev.*, **18** (3), 357 (1979).
10. J. Y. Oldshue, *Fluid Mixing Technology*, McGraw-Hill, NY, 1983, Chapter 7.
11. G. Baldi, R. Conti, and E. Alaria, *Chem. Eng. Sci.*, **33**, 21 (1978).
12. K. R. Westerterp, L. L. van Dierendonck, and J. A. de Kraa, *Chem. Eng. Sci.*, **18** 157 (1963).
13. *Chemical Engineer's Handbook*, 5th Ed., McGraw-Hill, NY 1973, Section 18-75.
14. S. V. Gollakota and J. A. Guin, *Ind. Eng. Chem. Proc. Des. Dev.*, **23**, 52 (1984).
15. S. I. El-Shawarby and S. H. Elssa, *Ind. Eng. Chem. Proc. Des. Dev.*, **19**, 469 (1980).
16. H. Yagi and F. Yoshida, *Ind. Eng. Chem. Proc. Des. Dev.*, **14** (4), 488 (1975).
17. J. B. Joshi and M. M. Sharma, *Can. J. Chem. Eng.*, **55**, 683 (1977).
18. H. Judat, *Ger. Chem. Eng.*, **5**, 357 (1982).
19. P. H. Calderbank, *Trans. Instn. Chem. Engrs.*, **37**, 173 (1959).
20. P. H. Calderbank and M. B. Moo-Young, *Chem. Eng. Sci.*, 16 (1), 39 (1961).
21. (a) T. Sridhar and O. E. Potter, *Ind. Eng. Chem. Fundam.*, **19**, 21 (1980); (b) T. Sridhar and O.E. Potter, *Chem. Eng. Sci.*, **35**, 683 (1980).
22. P. H. Calderbank, *Trans. Instn. Chem. Engrs.*, **36**, 443 (1958).
23. P. H. Calderbank, in *Mixing*, Vol. II, Chapter 6, edited by V. W. Uhl and J. B. Gray, Academic Press, 1967.
24. A. A. Kozinski and C. J. King, *AIChE J.*, **12** (1), 109 (1966).
25. J. C. Lamont and D. S. Scott, *AIChE J.*, **16** (4), 513 (1970).
26. F. Goodridge and D. J. Bricknell, *Trans. Instn. Chem. Engrs.*, **40**, 54 (1962).
27. R. E. Carpani and J. M. Roxburgh, *Can. J. Chem. Eng.*, April, 1958, 73.
28. A. I. Virozub, V. F. Kostenko, M. V. Lure, G. I. Papkov and B. G. Sheshev, *Khim. i Tex. Vodi, Akad. Nauk Ukr. C.C.P.*, 2 (2), 124 (1980).
29. G. T. N. Tsao, *Biotechnol. Bioeng.*, **7** (2), 177 (1968).
30. G. Quicker, A. Schumpe, and W. D. Deckwer, *Chem. Eng. Sci.*, **39** (1), 179 (1984).
31. G. E. H. Joosten, J. G. M. Schilder, and J. J. Janssen, *Chem. Eng. Sci.*, **32**, 563 (1977).
32. E. Alper and W. -D. Deckwer, in Mass Transfer with Chemical Reaction in Multi-phase Systems", Vol. II, Ed. by Erdogan Alper, NATO ASI Ser., Martinus Nijhoff, The Hague, 1983.
33. H. Kurten and P. Zehner, *Ger. Chem. Eng.*, **2**, 220 (1979).
34. (a) K.-H. Reichert and R. Michael, *I. Chem. E. Symp. Ser.*, **87**, 659 (1984); (b) R. Michael, Doctoral Thesis, Tech. Univ. Berlin (1984).
35. E. Alper, B. Wichtendahl, and W.-D. Deckwer, *Chem. Eng. Sci.*, **35**, 217 (1980).
36. J. H. Rushton, E. W. Costich, and H. J. Everett, *Chem. Eng. Prog.*, **46** (9), 467 (1950).
37. F. P. O'Connell and D. E. Mack, *Chem. Eng. Prog.*, **46** (7), 358 (1950).
38. B. J. Michel, and S. A. Miller, *AIChE J.*, **8** (2), 262 (1962).
39. "Stauffer Titanium Trichloride", Stauffer Chemical Co. Handbook, 1974.
40. U. S. P. 4,210,738, to Solvay and Cie. (Harmans et al.), 1980.
41. G. DiDrusco and L. Luciani, *J. Appl. Polym. Sci.*, **36**, 95 (1981).
42. R. B. Bird, W. E. Stewart, and E. N. Lightfoot, *Transport Phenomena*, Wiley, NY, 1960, p. 515.
43. J. L. Duda, J. S. Vrentas, S. T. Ju and H. T. Liu, *AIChE J.*, **28** (2), 279
44. S. U. Li and J. L. Gainer, *I. and E. C. Fundam.*, **7** (3), 433 (1968).
45. S. B. Clough, H. E. Read, A. B. Metzner and V. C. Behn, *AIChE J.*, **8** (3), 346 (1962).
46. R. M. Navari, J. L. Gainer, and K. R. Hall, *AIChE J.*, **17** (5), 1028 (1971).
47. T. W. Taylor, Ph.D. Thesis, University of Wisconsin (1983); G. E. Mann, M. S. Thesis, University of Wisconsin, (1985).
48. M. Benedict, G. B. Webb, and L. C. Rubin, *Chem. Eng. Prog.*, **47** (8), 419 (1951).
49. R. V. Orye, *I. &E.C. Proc. Des. Dev.*, **8** (4), 579 (1969).
50. W. B. Kay, *I. &E.C.*, **40** (2), 1459 (1948).
51. T. P. Zhuze and A. S. Zhurba, *Akad. Nauk. SSSR, Bull. Div. Chem. Sci.*, **335** (1960) (English translation).
52. M. Fujii, A. Matsui, and Y. Negami, *Polymer Preprints*, April 1985, p. 110.

53. H. Boerma, and J. H. Lankester, *Chem. Eng. Sci.*, **23**, 799 (1968).
54. L. L. Böhm, *Polymer*, **19**, 553 (1978).
55. M. N. Berger, and B. M. Grieveson, *Makromol. Chem.*, **83**, 80 (1965).
56. T. Furui, W. Zhixue and G. Peiyun, *J. Chem. Ind. and Eng.* (China) (Huagong Xuebao) **1**, 75 (1981).
57. "Selected Values of Physical and Thermodynamic Properties of Hydrocarbons and Related Compounds, A.P.R.I. Research Project 44, compiled by F. D. Rossini et al., Carnegie Press, Pittsburgh, PA, 1953.
58. *Chemical Engineer's Handbook*, 5th Ed., McGraw-Hill, NY 1973, Section 3-35.
59. R. W. Gallant, *Physical Properties of Hydrocarbons*, Vol. I, Gulf Press, Houston, 1968.
60. H. P. Frank, *Oesterr. Chem. Zeit.* (Vienna), **86**, 360 (1967).
61. B. Konobeev and V. Lyapin, *Khim. Prom.*, **43** (2), 114 (1967).

Received January 14, 1986
Accepted March 10, 1986